Journal of Engineering Science and Technology
Vol. 12, No. 2 (2017) 439 - 450

EQUIVALENT CIRCUIT MODEL OF OCTAGONAL ULTRA WIDEBAND (UWB) ANTENNA

LEE CHIA PING

School of Engineering, Taylor's University, Taylor's Lakeside Campus,
No. 1 Jalan Taylor's, 47500, Subang Jaya, Selangor DE, Malaysia
E-mail: ChiaPing.Lee@taylors.edu.my

Abstract

This paper presents an equivalent circuit model of an octagonal UWB antenna. The UWB antenna is first designed in the electromagnetic simulator, after which the circuit model is developed to match its result. The circuit model utilizes the concept of lumped elements, cascaded in stages, in which each represents the resonant part of the designed antenna element, thus contributing to the resonant frequencies. The antenna is also fabricated and the measured results are similar to that of the simulated results. This antenna also exhibits an impedance bandwidth from 2.7 GHz to 12 GHz, which covers the entire range of UWB characteristics from 3.1 GHz to 10.6 GHz.

Keywords: Equivalent circuit, Lumped element, Resonant frequency, Return Loss, S_{11}, Ultra wideband (UWB) antenna.

1. Introduction

The authorization of Federal Communications Commission (FCC) in 2002 for UWB frequency range between 3.1 GHz to 10.6 GHz has sparked great interest in the antenna industry [1]. UWB technology enables high data rate transmission which also prompts the research on antenna for various applications such as wireless communication, location tracking and imaging [2].

The design of UWB system comes with challenges, one of which is to obtain the equivalent circuit of the UWB antenna. The equivalent circuit of UWB antenna facilitates the understanding of antenna working [3], as well as matching potential of antenna such as calculation of limiting bandwidth with minimum achievable reflection coefficient [4].

Nomenclatures

h	Substrate thickness
k	Inductor coupling coefficient
LC	Resonant circuit
L_s	Surface inductance
L_{wi}	Inductance per unit length
M	Mutual coupling
R_s	Surface resistance
TEM	Transverse electromagnetic
Z_{om}	Characteristic impedance

Greek Symbols

λ	Wavelength
ε	Permittivity
S_{11}	Reflection coefficient
μ	Permeability

Abbreviations

FCC	Federal Communications Commission
UWB	Ultra Wideband
VSWR	Voltage Standing Wave Ratio

Research on equivalent circuit of antenna is reported in many literatures, though not extensively on UWB. Gerrits et al. designed an electrical equivalent schematic of dipole antenna but it only takes into account the first antenna resonance around 1.2 GHz, with its SPICE model having its limitation in time domain and extension to higher bandwidth [5]. Similar result is obtained by Long et al. [6], when their equivalent dipole circuit model exhibits fairly good fidelity up to first full-wave resonance but significant frequency and amplitude errors for higher order ones. A simple electrical model is proposed by Hafiane et al. [7] to determine the patch array antenna S-parameters which takes into account the coupling between the patches. Demeestere et al. modeled a short-circuited flat dipole antenna with lumped components *LC* network with the coupling between the microstrip line and short-circuited dipole represented by impedance transformer [3]. The antenna operates from 3 GHz to 7.5 GHz. Ghorbani et al. modeled the circuit of rectangular patch antenna with lumped element topology, giving good fit to the first resonance around 1 GHz but without attempt for higher resonances [4]. Wang and Li presented a paper on circuit refinement method by building a narrow-band model, augmented by macro-model to increase the accuracy of input admittance matching [8].

This paper presents an equivalent circuit model for an octagonal UWB antenna. A UWB antenna is first designed with a 3D electromagnetic simulator, ensued by the development of circuit model. Analysis is done to study the behaviour of the antenna elements made up from cascaded resonant circuits in the circuit simulator. The circuit model serves as a guide for design of UWB antennas while providing better insight of the antenna performance from the circuit point of view. The antenna is also fabricated and its measured results show good agreement with the simulated results.

2. Antenna Geometry

Figure 1 illustrates the geometry of UWB microstrip patch antenna. The proposed antenna comprises a radiator depicted as a symmetrical octagon shape, truncated from a larger rectangular patch, followed by a 50 Ohm microstrip feed line. The substrate used for the antenna designed is a Taconic TLC-30 board with relative permittivity of 3.0 and thickness of 1.575 mm. The radiator and feed line structure of antenna are designed on the front part of Taconic TLC-30 substrate. A partial ground plane with a slot is placed on the other side of the substrate. Simulations are done in optimizing the design parameters such as patch shape, feed line and ground plane before selecting the best dimensions to produce the best return loss, S_{11} and impedance bandwidth.

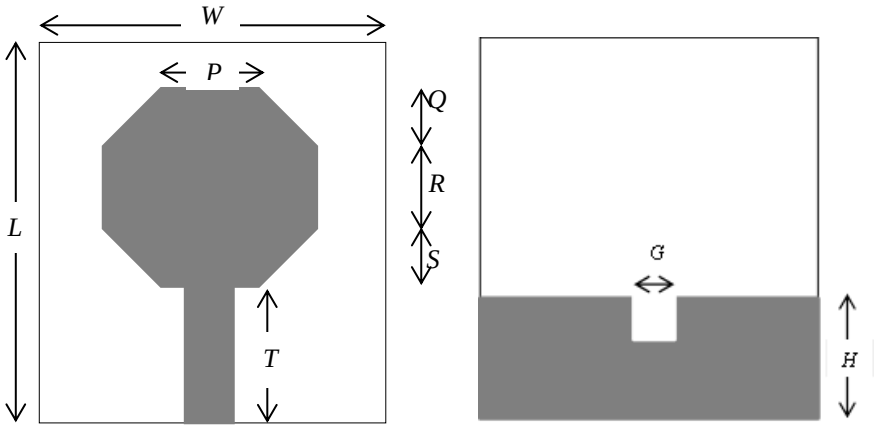

(a) Front configuration **(b) Back configuration**

Fig. 1. UWB antenna geometry.

The dimension of each design parameter is tabulated in Table 1.

Table 1. Dimension of antenna geometry.

Variable	Dimension (mm)
W	30
L	35
P	8
Q	5.3
R	8
S	5.3
T	11
G	4.2

3. Electromagnetic Simulation

Figure 2 illustrates the results of the return loss of the UWB antenna based on the electromagnetic simulation.

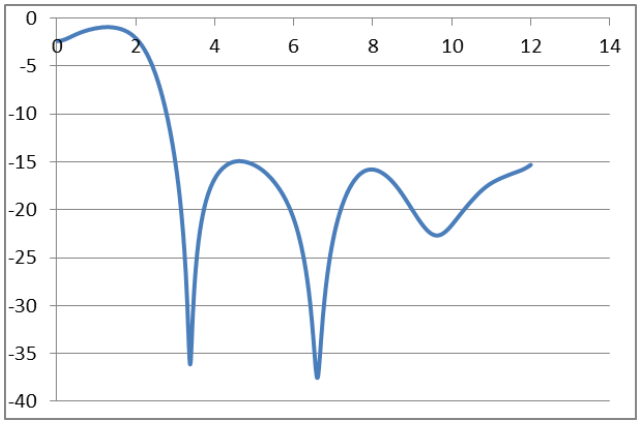

Fig. 2. Simulated return loss, S_{11} of UWB antenna using CST microwave studio.

Based on Fig. 2, it is observed that the modeled UWB antenna in the electromagnetic simulator exhibits very good return loss, S_{11} of below -15 dB throughout the operating frequency region. The UWB antenna operates with the impedance bandwidth from 2.7 GHz to 12 GHz. The antenna displays resonant frequencies at 3.38 GHz with S_{11} of -36.07 dB, 6.6 GHz with S_{11} of -37.53 dB and 9.68 GHz with S_{11} of -22.63 dB. The first resonant frequency is contributed by the patch length, L which also operates at TEM_{010} mode, given by Eq. (1).

$$f_{res,mnp} = \frac{1}{2\pi\sqrt{\mu\varepsilon}}\sqrt{\left(\frac{m\pi}{W}\right)^2 + \left(\frac{n\pi}{L}\right)^2 + \left(\frac{p\pi}{h}\right)^2} \quad (1)$$

The effective patch length, L is calculated to be at 0.4 λ, obtained by Eq. (2) [9]

$$\lambda = \frac{c}{f_r\sqrt{\varepsilon_{ref}}} \quad (2)$$

where λ is the wavelength, c is speed of light, f_r is resonant frequency and ε_{ref} is the dielectric constant.

Each part of the patch shape affects the performance of the antenna in terms of S_{11} and impedance bandwidth. The upper slant of the octagon shaped antenna, 'Q' contributes to lowering the peaks depicted in Fig. 2 to better S_{11} reading and shifting of the first resonant frequency to the left, thereby extending the impedance bandwidth. The second resonant frequency observed is due to the lower slant of the patch, 'S' as shown in Fig. 1. The truncated lower slant leads to abrupt change of the patch antenna geometry which consequently causes discontinuity in the microstrip line [10]. The fact that the lower slant is positioned near the partial ground plane also tunes the capacitive coupling between the two, thus increasing the impedance bandwidth. The partial ground plane is constructed in such that the graph could be brought down to less than -10 dB. However, a slot is placed in the middle of the partial ground plane to introduce the third resonant frequency in the graph, in order to achieve the FCC's release of UWB operating bandwidth from 3.1 GHz to 10.6 GHz.

4. Equivalent Circuit Model

The development of equivalent circuit model of the antenna is based on the microstrip line cavity model, comprising lumped elements. For the proposed antenna, each stage of the equivalent circuit model comprises a resistor and inductor in series with an *LC* paired parallel to produce oscillation at its resonant frequency. From literature [11], the resistor and inductor in series represent the surface resistance, R_s and surface inductance, L_s given by the equation as follow

$$R_s = \frac{1}{w\sigma_{cond}\delta} \tag{3}$$

$$L_s = \frac{1}{w\sigma_{cond}\omega\delta} \tag{4}$$

where σ_{cond} is the conductivity, w is the width, ω is angular frequency and δ is the skin depth.

Meanwhile, the parallel *LC* circuit is expressed with its variables computed using the quasi-static method as shown in [11]

$$C_s = 0.00137\frac{\sqrt{\varepsilon_{re1}}}{Z_{om1}}\left(1-\frac{W_2}{W_1}\right)h\left[\frac{\varepsilon_{re1}+0.3}{\varepsilon_{re1}-0.258}\right]\left[\frac{\frac{W_1}{h}+0.264}{\frac{W_1}{h}+0.8}\right](pF) \tag{5}$$

$$L_1 = \frac{L_{w1}}{L_{w1}+L_{w2}}L_s \tag{6}$$

$$L_2 = \frac{L_{w2}}{L_{w1}+L_{w2}}L_s \tag{7}$$

$$L_{wi} = \frac{Z_{om}\sqrt{\varepsilon_{re}}}{c}\ (H/m) \tag{8}$$

$$L_s = 0.000987h\left(1-\frac{Z_{om1}}{Z_{om2}}\sqrt{\frac{\varepsilon_{re1}}{\varepsilon_{re2}}}\right)^2(nH) \tag{9}$$

where L_{wi} for i=1, 2 indicate inductance per unit length of microstrip of widths W_1 and W_2, while Z_{om} and $\boldsymbol{\varepsilon}_{re}$ indicate the microstrip line characteristic impedance and effective dielectric constant, respectively, and the substrate thickness h is in micrometers.

The microstrip discontinuity equivalent circuit is as illustrated in Fig. 3.

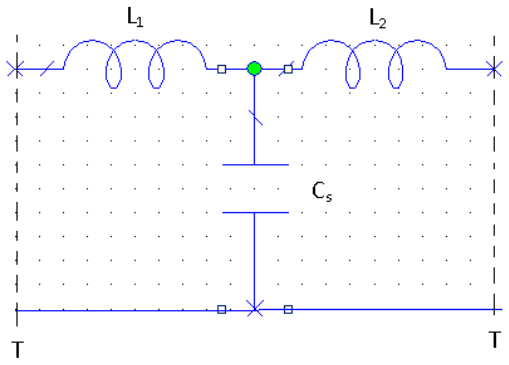

Fig. 3. Microstrip discontinuity equivalent circuit.

The equivalent circuit model for the proposed UWB antenna is first developed as three cascaded stages of resonant circuit illustrated in Fig. 4. A tuning capacitor precedes the resonant circuits to correctly reproduce the low frequency behavior [4] by improving the reactance representation [6]. The mutual coupling between the inductors for each stage is also taken into account following the equation:

$$M = k\sqrt{L_1 L_2} \tag{10}$$

where k is the inductor coupling coefficient and L_1 and L_2 being the inductors.

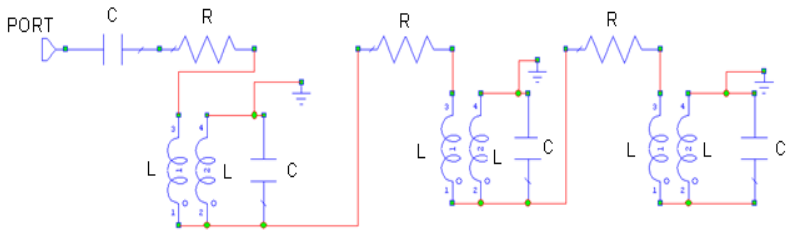

Fig. 4. Equivalent circuit model for the proposed UWB antenna.

The equivalent circuit model in Fig. 4 is developed using the circuit simulator software to match the result obtained in Fig. 2 from the electromagnetic simulator. The comparison between both results is illustrated in Fig. 5.

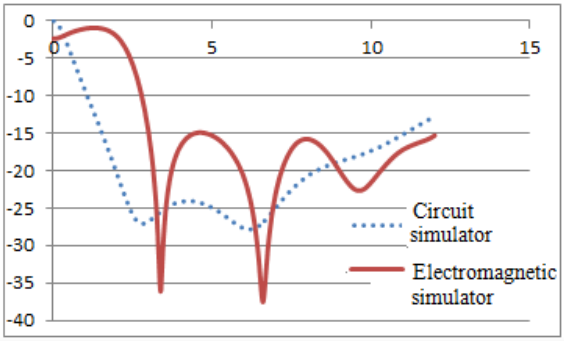

Fig. 5. Simulated return loss, S_{11} for Fig. 4 compared to electromagnetic simulator.

The first resonant frequency is contributed by the first stage of the circuit as seen in Fig. 4, representing the antenna patch length modeled in the electromagnetic simulator. Even though the three cascaded resonant circuit in Fig. 4 is to produce three resonant frequencies, the best optimization done has led to the finding that the second resonant frequency observed in Fig. 5 could be obtained around the 6.6 GHz only with the contribution of the second and third stage of the resonant circuit. The optimized second stage circuit is at its resonance at 8 GHz and combining the third stage solves the problem by bringing it closer to 6.6 GHz. This solution works by having two resonant modes which are close to each other that it strongly overlaps [12], merging into one frequency, which can also be thought of as 'near-degenerate' modes. This indicates that the equivalent circuit in Fig. 4 only manages to produce two resonant frequencies, and even as

compared to the result in the electromagnetic simulator, is unable to reproduce a similar result as the former. As reported in [6], additional lumped components reduce the error of obtaining higher resonance. Thus, improvisation is done by cascading another resonant circuit which is illustrated in Fig. 6.

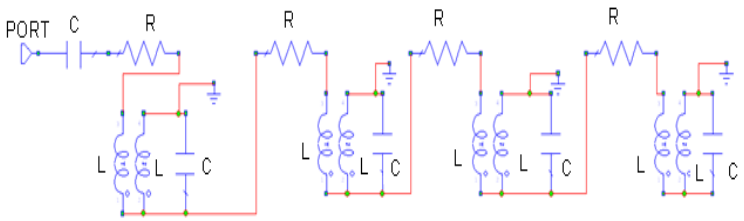

Fig. 6. The best modeled equivalent circuit for the proposed UWB antenna.

The simulated return loss of the equivalent circuit is compared to electromagnetic simulator as depicted in Fig. 7. It is observed that the result obtained from the circuit model simulation matches very well with that of the 3D electromagnetic simulator for the antenna structure. As depicted in the graph, the equivalent circuit model exhibits resonant frequencies at 3.087 GHz with S_{11} of -36.08 dB, 6.59 GHz with S_{11} of -37.53 dB and 9.813 GHz with S_{11} of -22.47 dB. The percentage of difference for each resonant frequency between both methods is calculated to be 8.67%, 0% and 1.37%. Based on the circuit model, the first stage of resonant circuit represents the patch length as it affects the first resonant frequency seen in the return loss, S_{11} graph. The patch upper slant denoted as '*Q*' in Fig. 1 plays a role in the inductor values for stage one, validated by the fact that it does affect the shifting of the first resonant frequency. The second and third stages represent the second resonant frequency which is contributed by the patch lower slant, '*S*'. As discussed earlier, the patch lower slant structure tunes the capacitive coupling between the patch antenna and the ground plane and wider impedance bandwidth is achieved. In this case, electric and magnetic field distributions are modified near the discontinuity when the geometry of antenna changes. The altered electric field distribution gives rise to a change in capacitance, and the changed magnetic field distribution can be expressed in terms of an equivalent inductance. The last stage of the resonant circuit represents the slot at the ground plane.

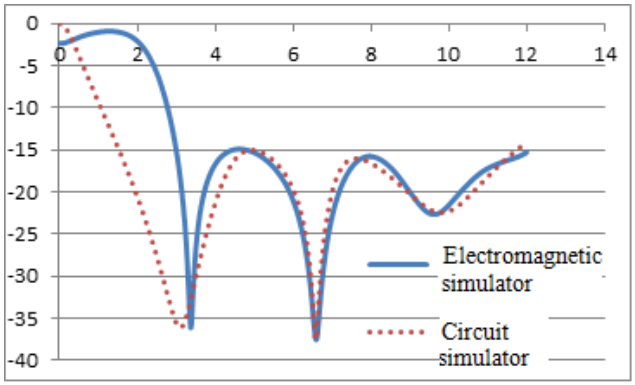

Fig. 7. Comparison of return loss, S_{11} between circuit and electromagnetic simulator.

5. Fabricated Antenna

The proposed antenna is fabricated for its measurement, as illustrated in Fig. 8. It is noted that the simulations involved the antenna being fed at the end of the feed line of the antenna structure, whereas the measurement was done using Rohde&Schwarz R&S®ZVB20 network analyser with its RF cable connecting to the SMA connector soldered on the antenna as illustrated in Fig. 8.

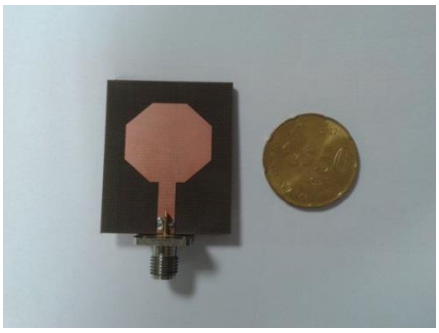

Fig. 8. Fabricated antenna.

Figure 9 illustrates the simulated and measured return loss of the antenna. Both results show good similarity with the measured result depicting its resonant frequencies shifted slightly to the left. The first resonant frequency is at 2.93 GHz with S_{11} of -31.1 dB, followed by the second resonant frequency at 6.23 GHz with S_{11} of -48.9 dB and finally 9.6 GHz with S_{11} of -18.3 dB. The percentage of difference of the resonant frequencies between both results is the highest for the first resonant, recording a 13.3% difference, followed by 5.6% for the second and 0.8% for the third. The fabricated antenna also exhibits the impedance bandwidth from 2.06 GHz to 12 GHz, which is very satisfactory. The slight ripples and shifting of the measured result compared to the simulated one could be due to the fabrication tolerances. As UWB antenna is very sensitive, any misalignment of the patch and ground would contribute to the different result. Besides, there could be some losses in the measured result due to the SMA connector being soldered onto the antenna substrate, which is unaccounted for in the theoretical result. Measurement with RF cable usually affects the performance of antenna under test [13], which could also explain the ripples for the measured result due to the factor of the length of the inner conductor for the feeding RF cable.

Table 2 summarizes the shift in resonant frequencies discussed for the electromagnetic simulator, circuit simulator and measured results.

Table 2. Shifting of resonant frequencies for simulated and measured results.

Theoretical Simulation/Measured Results	**Resonant Frequencies (GHz)**		
	f_1	f_2	f_3
Electromagnetic	3.380	6.600	9.680
Circuit	3.087	6.590	9.813
Measured	2.930	6.230	9.600

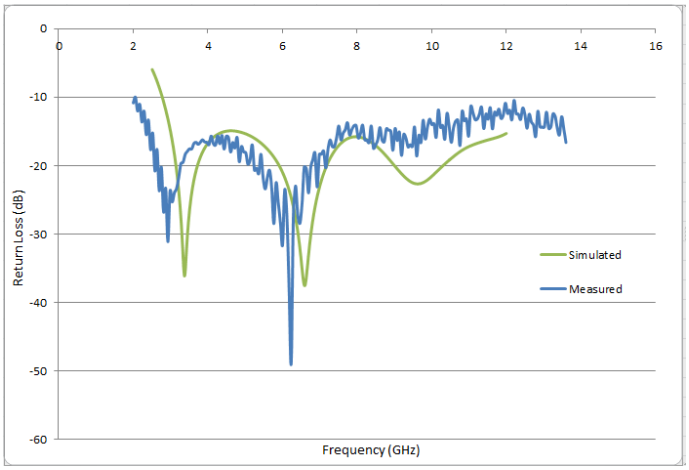

Fig. 9. Simulated and measured return loss.

Figure 10 illustrates the simulated and measured voltage standing wave ratio (VSWR) of the antenna. It depicts the range of VSWR between 1 and 2 across the frequency range from 2.7 GHz to 12 GHz for the simulated result, whereas the measured result shows similar pattern from 2.06 GHz to 12 GHz. UWB characteristics requires the return loss of below -10 dB across its operating frequencies and it is indicated by VSWR from 1 to 2. Thus, the VSWR results validate well with the return loss results as seen in Fig. 9.

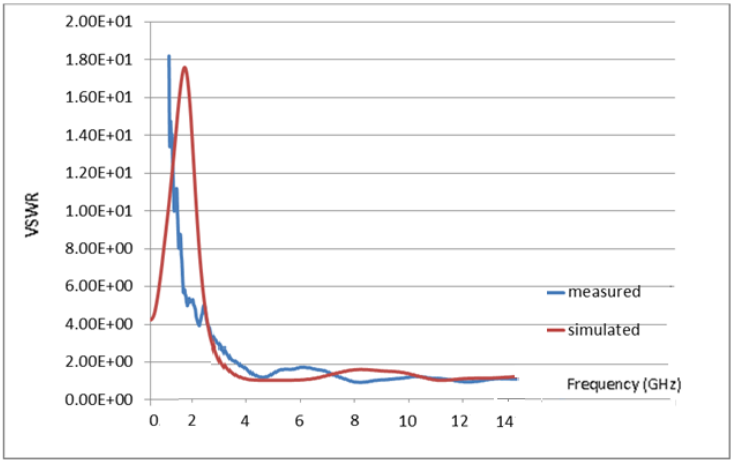

Fig. 10. Simulated and measured VSWR.

Figures 11 and 12 illustrate the radiation patterns of the antenna in terms of *E*-plane and *H*-plane respectively. Based on Fig. 11, it could be observed that the antenna displays a directional pattern with its concentration focusing on the sides of the patch antenna. It could be seen that the radiation patterns are suppressed at 90º and 270º, with increasing directivity with increasing frequency, probably due to the propagation of higher mode order. As of the *H*-plane, the patterns exhibit omnidirectional patterns throughout the frequency except for 9-GHz, which is expected.

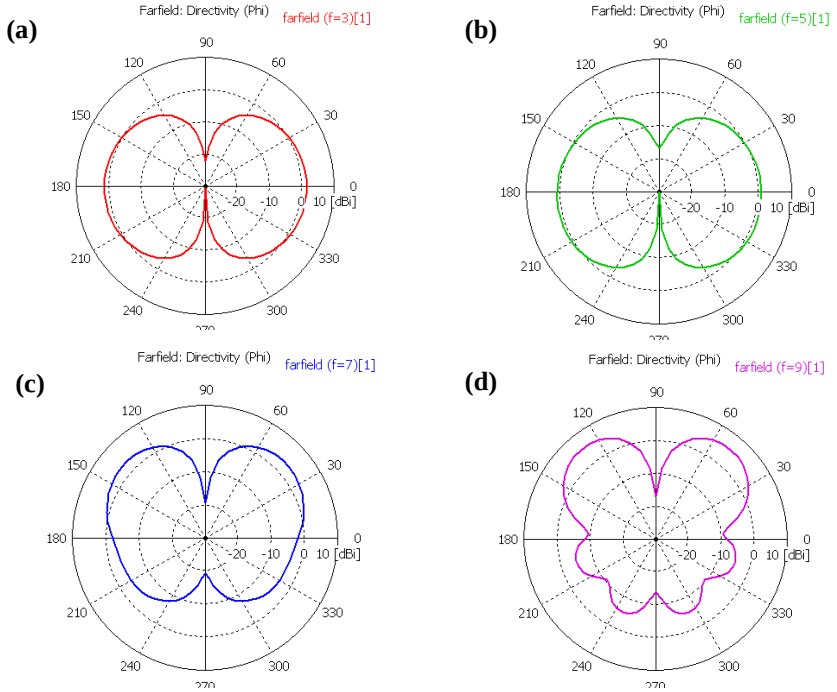

Fig. 11. Radiation patterns of *E*-plane directivity at (a) 3 GHz (b) 5 GHz (c) 7 GHz (d) 9 GHz.

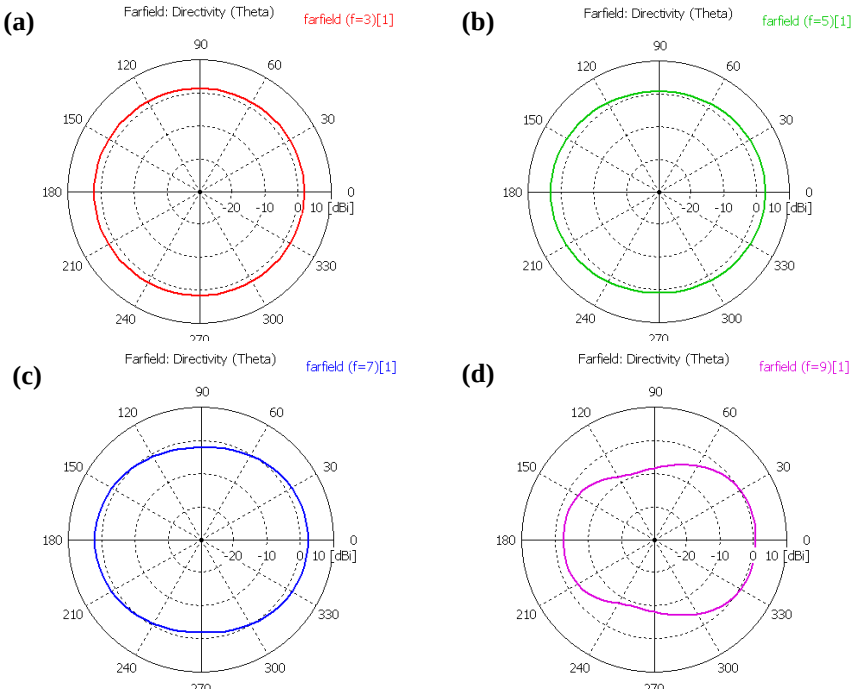

Fig. 12. Radiation patterns of *H*-plane at directivity (a) 3 GHz (b) 5 GHz (c) 7 GHz (d) 9 GHz.

This research validates the circuit modeling of the designed UWB antenna with its simplistic design and yet is able to exhibit impedance bandwidth from 2.7 GHz to 12 GHz. This design actually surpasses the coverage of bandwidth designed by Matin et al. [14], in their stacked configuration of antenna which operates from 3.06 to 5.49 GHz. Douyere et al. [15] produced an equivalent circuit approach but only focusing on narrowband antenna, while this research develops an equivalent circuit for UWB antenna. The development of the circuit model provides an insight on designed antenna from circuit viewpoint, and would aid in reducing the time taken to design antenna in electromagnetic simulator, due to the fact that the behavior of the antenna is known, and therefore could be adjusted accordingly in its electromagnetic simulation.

6. Conclusion

An equivalent circuit model is developed for an octagonal UWB antenna in this paper. The antenna is designed in such way that it matches the results obtained from 3D electromagnetic simulator. The circuit model comprises cascaded resonant circuits, each of which represents the resonant part of the antenna element, thus producing a resonant frequency. The results obtained from both electromagnetic and circuit simulators are with good agreement with one another, as well as the measured results. It is observed how truncation of the microstrip lines or discontinuity of the antenna geometry contributes to the respective resonant frequencies, giving rise of change in terms of its electric and magnetic field distributions of the antenna elements. This electromagnetic analysis is supported by the circuit model which discusses how the resonant components contribute to the results based on the lumped elements. This model provides good approximation of antenna behavior in its UWB performance, particularly with the capacitance related to the electric field and inductance to the magnetic field, from the circuit point of view. The designed antenna only exhibits good measured result and thus, is suitable for UWB applications.

References

1. Siriwongpairat, W.P.; and Ray Liu, K.J. (2007). *Ultra-wideband communication system: Multiband OFDM approach* (*Wiley series in telecommunications & signal processing*). John Wiley & Sons Publication, Hoboken, New Jersey.
2. Chen, Z.N. (2007). UWB antenna design and application. *International Conference on Information & Communication Systems* 2007, 1-5, Singapore.
3. Demeestere, F.; Delaveaud, C.; and Keignart, J. (2006). A compact UWB antenna with a wide band circuit model and a time domain characterization. *IEEE 2006 International Conference on Ultra-Wideband*, 345-350, Waltham, Massachusetts.
4. Ghorbani, A.; and Abd-Alhameed, R.A. (2006). An approach for calculating the limiting bandwidth - Reflection coefficient product for microstrip patch antennas. *IEEE Transactions on Antennas and Propagation*, 54(4), 1328-1331.
5. Gerrits, J.F.M.; Hutter, A.A., Ayadi, J.; and Farserotu, J.R. (2003) Modeling and simulation of a dipole antenna for UWB applications using equivalent

SPICE circuits. *Proceedings of the 2003 International Workshop on Ultra Wideband System*s, Oulu, Finland.

6. Long, B.; Werner, P.; and Werner, D. (2000). A simple broadband dipole equivalent circuit model. *IEEE 2000 Antennas and Propagation Society International Symposium*, vol.2, pp.1046- 049, Salt Lake City, UT, USA.
7. Hafiane, A.; Aissat, H.; and Picon, O. (2003). Simple electrical model to calculate patch array antenna S-parameters. *Electronics Letters*, 39(14), 1031-1033.
8. Wang, Y.; Li, J.Z.; and Ran, L.-X. (2008). An equivalent circuit modeling method for ultra-wideband antennas. *PIER - Progress in Electromagnetics Research*, 82, 433-445.
9. Amaro, N.; Mendes, C.; and Pinho, P. (2011) Bending effects on a textile microstrip antenna. *2011 IEEE International Symposium on Antennas and Propagation (APSURSI)*, 282 - 285, Spokane, WA.
10. Gupta, K.C.; Garg, R.; Bahl, I.; and Bhartia, P. (1996). *Microstrip lines and slotlines*. Artech House, 2nd Ed, Norwood, MA.
11. Ludwing, R.; and Bretchko, P. (2000). *RF circuit design.* Prentice Hall, New Jersey, United States of America.
12. Lo, Y.T.; and Lee, S.W. (1993). *Antenna handbook, Vol. 2 Theory.* Van Nostrand Reinhold, New York, United States of America.
13. Chen, Z.N. (2007). *Antenna for portable device*. John Wiley & Sons Ltd, England.
14. Matin, M.A.; Sharif, B.S.; and Tsimenidis, C.C. (2007). Dual layer stacked rectangular microstrip patch antenna for ultra wideband applications. *IET Microwaves, Antennas & Propagation*, 1(6), 1192-1196.
15. Douyere, A.; Lan Sun Luk, J.D.; and Alicalapa, F. (2008). High efficiency microwave rectenna circuit: modelling and design. *Electronics Letters*, 44(24), 1409-1410.